Acta Cryst E CRYSTALLOGRAPHIC COMMUNICATIONS

ISSN 2056-9890

2-{(1*E*)-[(*E*)-2-(2,6-Dichlorobenzylidene)hydrazin-1-ylidene]methyl}phenol: crystal structure, Hirshfeld surface analysis and computational study

Rohit B. Manawar,[a] Mitesh B. Gondaliya,[a] Manish K. Shah,[a]‡ Mukesh M. Jotani[b] and Edward R. T. Tiekink[c]*

[a]Chemical Research Laboratory, Department of Chemistry, Saurashtra University, Rajkot - 360005, Gujarat, India, [b]Department of Physics, Bhavan's Sheth R. A. College of Science, Ahmedabad, Gujarat - 380001, India, and [c]Research Centre for Crystalline Materials, School of Science and Technology, Sunway University, 47500 Bandar Sunway, Selangor Darul Ehsan, Malaysia. *Correspondence e-mail: edwardt@sunway.edu.my

Received 3 September 2019
Accepted 4 September 2019

Edited by W. T. A. Harrison, University of Aberdeen, Scotland

‡ Additional correspondence author, email: drmks2000hotmail.com.

Keywords: crystal structure; Schiff base; Hirshfeld surface analysis; computational chemistry.

CCDC reference: 1857868

Supporting information: this article has supporting information at journals.iucr.org/e

The title Schiff base compound, $C_{14}H_{10}Cl_2N_2O$, features an *E* configuration about each of the C=N imine bonds. Overall, the molecule is approximately planar with the dihedral angle between the central C_2N_2 residue (r.m.s. deviation = 0.0371 Å) and the peripheral hydroxybenzene and chlorobenzene rings being 4.9 (3) and 7.5 (3)°, respectively. Nevertheless, a small twist is evident about the central N—N bond [the C—N—N—C torsion angle = −172.7 (2)°]. An intramolecular hydroxy-O—H···N(imine) hydrogen bond closes an *S*(6) loop. In the crystal, π–π stacking interactions between hydroxy- and chlorobenzene rings [inter-centroid separation = 3.6939 (13) Å] lead to a helical supramolecular chain propagating along the *b*-axis direction; the chains pack without directional interactions between them. The calculated Hirshfeld surfaces point to the importance of H···H and Cl···H/H···Cl contacts to the overall surface, each contributing approximately 29% of all contacts. However, of these only Cl···H contacts occur at separations less than the sum of the van der Waals radii. The aforementioned π–π stacking interactions contribute 12.0% to the overall surface contacts. The calculation of the interaction energies in the crystal indicates significant contributions from the dispersion term.

1. Chemical context

Being deprotonable and readily substituted with various residues, Schiff base molecules are prominent as multidentate ligands for the generation of a wide variety of metal complexes. In our laboratory, a key motivation for studies in this area arises from our interest in the Schiff bases themselves and of their metal complexes, which are well-known to possess a wide spectrum of biological activity against disease-causing microorganisms (Tian *et al.*, 2009; 2011). Over and beyond biological considerations, Schiff bases are also suitable for the development of non-linear optical materials because of their solvato-chromaticity (Labidi, 2013).

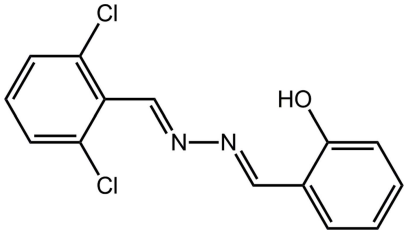

As reported recently, the title compound, (I), a potentially multidentate ligand has anti-bacterial and anti-fungal action

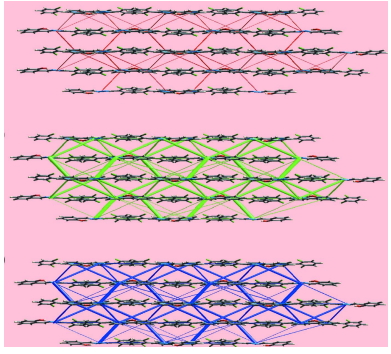

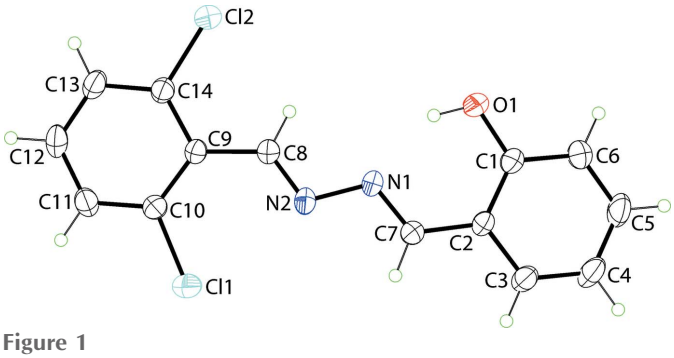

Figure 1
The molecular structure of (I) showing the atom-labelling scheme and displacement ellipsoids at the 35% probability level.

against a range of microorganisms (Manawar *et al.*, 2019). As a part of complementary structural studies on these molecules, the crystal and molecular structures of (I) are described herein together with a detailed analysis of the calculated Hirshfeld surfaces.

2. Structural commentary

The title Schiff base molecule (I), Fig. 1, features two imine bonds, C7═N1 [1.281 (2) Å] and C8═N2 [1.258 (3) Å] with the configuration about each being *E*. The central N1, N2, C7, C8 chromophore is close to being the planar, exhibiting an r.m.s. deviation of 0.0371 Å, with deviations of 0.0390 (11) and 0.0372 (10) Å above and below the means plane for the N1 and C7 atoms, respectively. There is a small but significant twist about the central N1—N2 bond [1.405 (2) Å] as seen in the value of the C7—N1—N2—C8 torsion angle of −172.7 (2)°. The dihedral angles between the central plane and those through the hydroxybenzene [4.9 (3)°] and chlorobenzene [7.5 (3)°] rings, respectively, and that between the outer rings [4.83 (13)°] indicate that to a first approximation, the entire molecule is planar. An intramolecular hydroxy-O—H···N(imine) hydrogen bond is noted, Table 1, which closes an *S*(6) loop.

Table 1
Hydrogen-bond geometry (Å, °).

D—H···*A*	*D*—H	H···*A*	*D*···*A*	*D*—H···*A*
O1—H1O···N1	0.87 (3)	1.87 (3)	2.632 (2)	147 (3)

3. Supramolecular features

The most prominent supramolecular association in the crystal of (I) are π–π stacking interactions. These occur between the hydroxy- and chlorobenzene rings with an inter-centroid separation = 3.6939 (13) Å and angle of inclination = 4.32 (11)° [symmetry operation $\frac{3}{2} - x, \frac{1}{2} + y, \frac{1}{2} - z$]. As these interactions occur at both ends of the molecule and are propagated by screw-symmetry (2_1), the topology of the resultant chain is helical, Fig. 2(*a*). According to the criteria

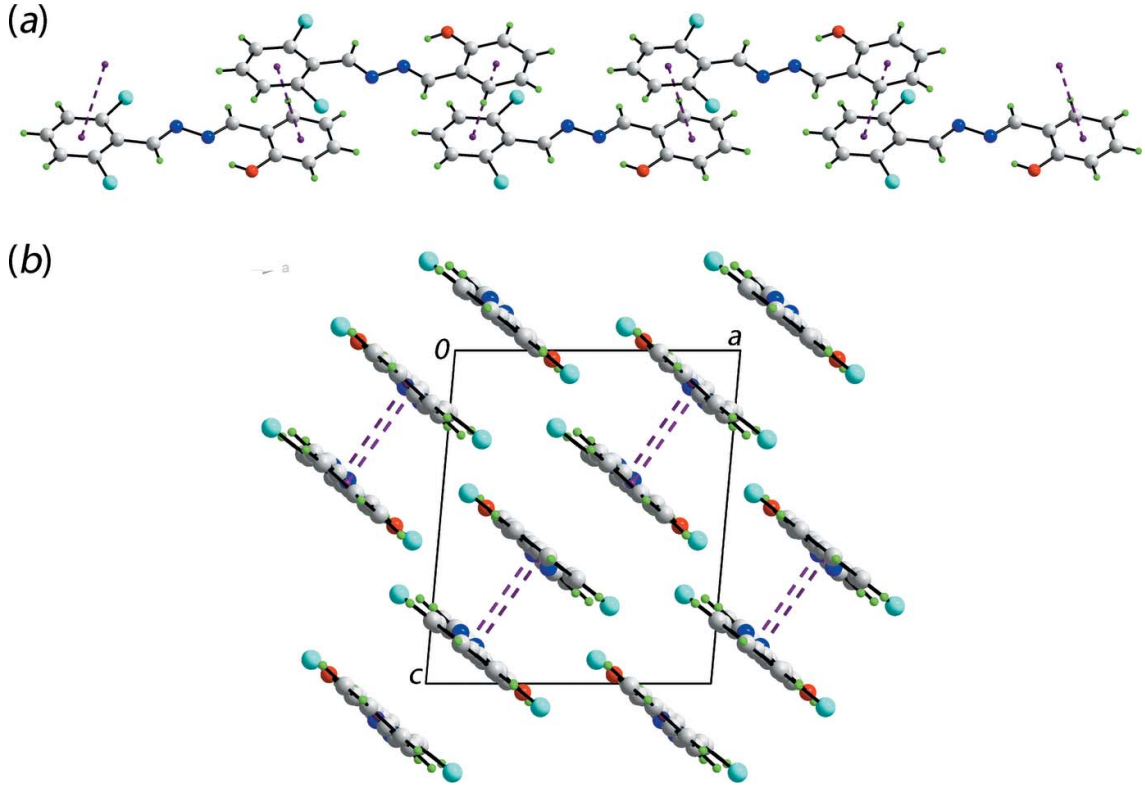

Figure 2
Molecular packing in the crystal of (I): (*a*) supramolecular chain sustained by π(hydroxybenzene)–π(chlorobenzene) interactions shown as purple dashed lines and (*b*) a view of the unit-cell contents in a projection down the *b* axis.

Table 2
Summary of short interatomic contacts (Å) in (I)[a].

Contact	Distance	Symmetry operation
Cl1···H6	2.86	$-\frac{1}{2}+x, \frac{1}{2}-y, -\frac{1}{2}+z$
Cl2···H4	2.85	$\frac{1}{2}+x, \frac{1}{2}-y, \frac{1}{2}+z$
O1···H7	2.68	$\frac{1}{2}+x, \frac{1}{2}-y, \frac{1}{2}+z$
C2···C12	3.399 (3)	$1-x, -y, 1-z$

Note: (*a*) The interatomic distances were calculated using *Crystal Explorer 17* (Turner *et al.*, 2017) whereby the *X*—H bond lengths are adjusted to their neutron values.

incorporated in *PLATON* (Spek, 2009), there are no directional interactions connecting chains; a view of the unit-cell contents is shown in Fig. 2(*b*). The presence of other, weaker points of contact between atoms and between residues are noted – these are discussed in more detail in *Hirshfeld surface analysis.*

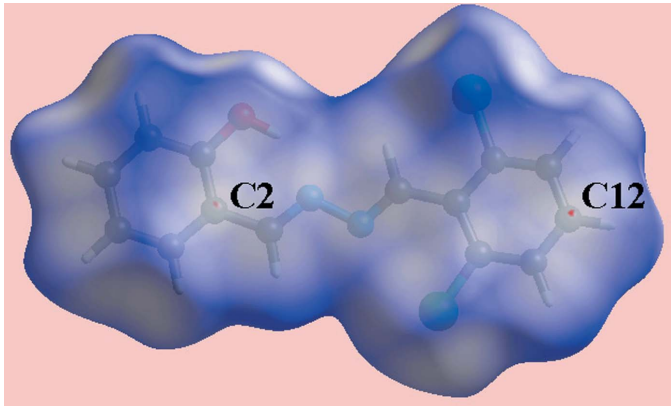

Figure 3
A view of the Hirshfeld surface for (I) mapped over d_{norm} in the range −0.001 to + 1.301 (arbitrary units), highlighting diminutive red spots near the C2 and C12 atoms owing to their participation in C···C contacts.

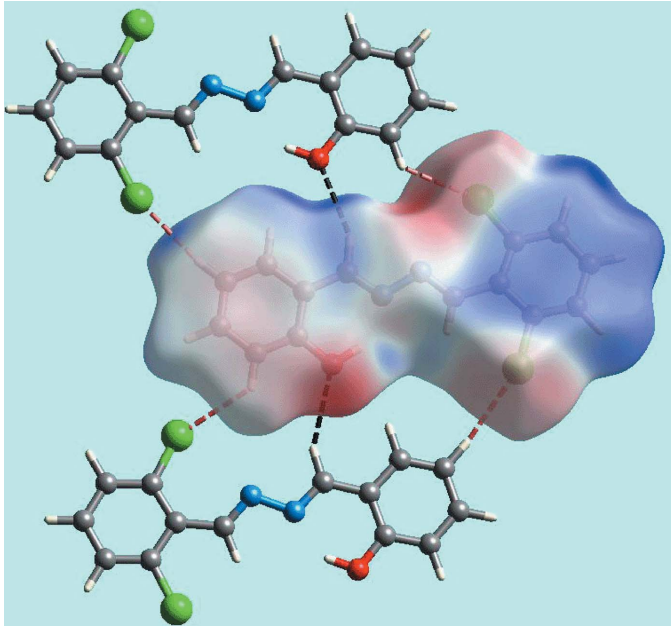

Figure 4
A view of the Hirshfeld surface mapped over the electrostatic potential (the red and blue regions represent negative and positive electrostatic potentials, respectively) in the range −0.065 to + 0.039 atomic units, with short interatomic Cl···H and O···H contacts highlighted with red and black dashed dashed lines, respectively.

Table 3
Percentage contributions of interatomic contacts to the Hirshfeld surface for (I).

Contact	Percentage contribution
H···H	29.4
Cl···H/H···Cl	29.1
O···H/H···O	7.4
C···H/H···C	12.0
C···C	12.0
N···H/H···N	4.5
C···N/N···C	3.9
C···Cl/Cl···C	0.6
Cl···Cl	0.4
Cl···N/N···Cl	0.4
Cl···O/O···Cl	0.1
C···O/O···C	0.1

4. Hirshfeld surface analysis

The Hirshfeld surface calculations for (I) were performed employing *Crystal Explorer 17* (Turner *et al.*, 2017) and recently published protocols (Tan *et al.*, 2019). On the Hirshfeld surface mapped over d_{norm} in Fig. 3, the short interatomic contact between the hydroxyphenyl-C2 and chlorophenyl-C12 atoms (Table 2) is characterized as small red spots near them. The Cl1 and Cl2 atoms form short intra-layer Cl···H contacts with the H4 and H6 atoms of the hydroxyphenyl ring (Table 2) and are represented in Fig. 4, showing a reference molecule within the Hirshfeld surface mapped over the electrostatic potential. The Hirshfeld surface mapped with curvedness is shown in Fig. 5, which highlights the influence of the short interatomic C···C contacts in the packing (Table 2) consistent with the edge-to-edge π–π stacking between symmetry related molecules.

The full two-dimensional fingerprint plot for (I), Fig. 6(*a*), and those decomposed into H···H, O···H/H···O, Cl···H/H···Cl, C···C and C···H/H···C contacts are illustrated in Fig. 6(*b*)-(*f*), respectively. The percentage contributions from the different interatomic contacts to the Hirshfeld surface of (I) are quantitatively summarized in Table 3. It is evident from

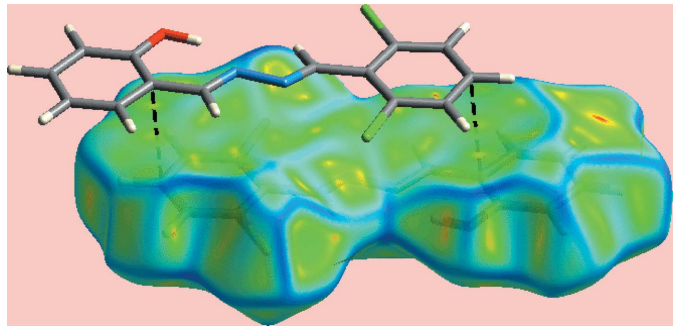

Figure 5
A view of Hirshfeld surface mapped with curvedness showing edge-to-edge π–π overlap through black dashed lines.

Table 4
Summary of interaction energies (kJ mol^{-1}) calculated for (I).

Contact	R (Å)	E_{ele}	E_{pol}	E_{dis}	E_{rep}	E_{tot}
C2···C12^{i}	4.00	−13.1	−1.4	−77.2	42.7	−55.8
Cg(C1–C6)···Cg(C9–C14)^{ii}	8.58	−5.9	−0.9	−40.1	20.6	−29.2
Cl1···H6^{iii} + Cl2···H4^{iv} + O1···H7^{iv}	8.53	−10.4	−1.8	−20.9	19.1	−18.7

the fingerprint plot delineated into H···H contacts in Fig. 6(*b*) that their interatomic distances are equal to or greater than the sum of their respective van der Waals radii. The fingerprint plot delineated into O···H/H···O contacts in Fig. 6(*c*) indicates the presence of short interatomic O···H contacts involving hydroxy-O1 and phenyl-H7 atoms through the pair of forceps-like tips at $d_e + d_i < 2.7$ Å. The presence of a pair of conical tips at $d_e + d_i \sim 2.9$ Å in the fingerprint plot delineated into Cl···H/H···Cl contacts in Fig. 6(*d*) are due to the Cl···H contacts listed in Table 2. In the fingerprint plot decomposed into C···C contacts in Fig. 6(*e*), the π–π stacking between symmetry-related hydroxy- and chlorobenzene rings are characterized as the pair of small forceps-like tips at $d_e + d_i \sim 3.4$ Å together with the green points distributed around $d_e = d_i \sim 1.8$ Å. The fingerprint plot delineated into C···H/H··· C contacts in Fig. 6(*f*) confirms the absence of significant C—H···π and C···H/H···C contacts as the points in the respective delineated plot are distributed farther than sum of their respective van der Waals radii. The small contribution from other interatomic contacts to the Hirshfeld surfaces of (I) summarized in Table 3 have a negligible effect on the molecular packing.

5. Computational chemistry

In the present analysis, the pairwise interaction energies between the molecules in the crystal were calculated by summing up four different energy components (Turner *et al.*, 2017). These comprise electrostatic (E_{ele}), polarization (E_{pol}), dispersion (E_{dis}) and exchange–repulsion (E_{rep}), and were obtained using the wave function calculated at the B3LYP/6-31G(d,p) level of theory. From the intermolecular interaction energies collated in Table 4, it is apparent that the dispersion energy component has a major influence in the formation of the supramolecular architecture of (I) as conventional hydrogen bonding is absent. The energy associated with the π–π stacking interaction between symmetry-related hydroxy- and chlorobenzene rings is greater than the energy calculated for the Cl···H/H···Cl and O···H/H···O contacts. The magnitudes of intermolecular energies were also represented graphically in Fig. 7 by energy frameworks whereby the cylinders join the centroids of molecular pairs using a red, green and blue colour scheme for the E_{ele}, E_{disp} and E_{tot} components, respectively; the radius of the cylinder is proportional to the magnitude of interaction energy.

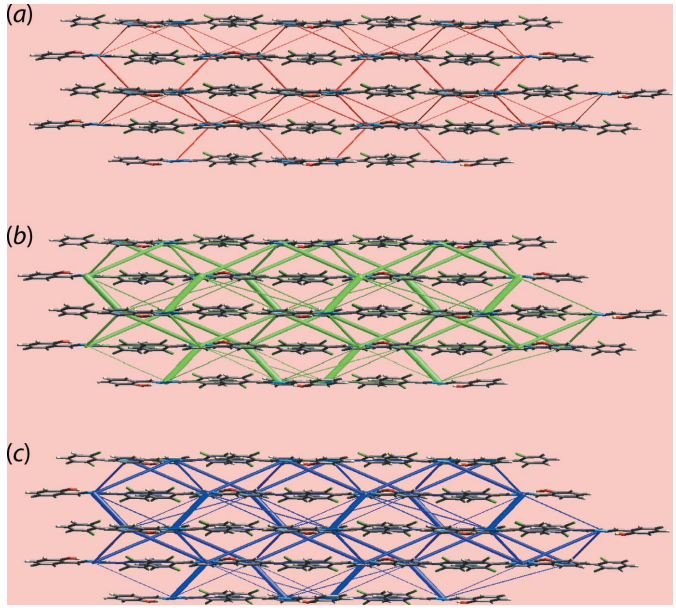

Figure 7
The energy frameworks calculated for (I) showing the (*a*) electrostatic potential force, (*b*) dispersion force and (*c*) total energy. The energy frameworks were adjusted to the same scale factor of 50 with a cut-off value of 5 kJ mol^{-1} within 4 × 4 × 4 unit cells

6. Database survey

Given the great interest in Schiff bases and their complexation to transition metals and other heavy elements, it is not surprising that there is a wealth of structural data for these compounds in the Cambridge Structural Database (CSD; Groom *et al.*, 2016). Indeed, there are over 150 'hits' for the basic framework 2-OH-C$_6$—C═N—N═C—C$_6$ featured in

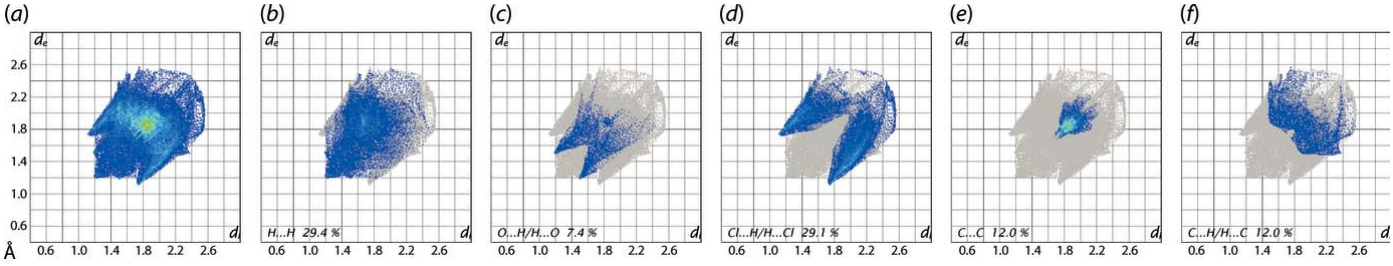

Figure 6
(*a*) A comparison of the full two-dimensional fingerprint plot for (I) and those delineated into (*b*) H···H, (*c*) O···H/H···O, (*d*) Cl···H/H···Cl, (*e*) C···C and (*f*) C···H/H···C contacts.

Table 5
Geometric data (°) for related 2-OH−C_6−C(H)=N−N=C(H)−C_6 molecules, *i.e.* R^1−C(H)=N−N=C(H)−R^2.

Compound	R^1	R^2	C−N−N−C	C_2N_2/*R*-C_6	C_2N_2/*R*′-C_6	*R*-C_6/*R*′-C_6	REFCODE
(I)	2-OH−C_6H_4	2,6-Cl_2−C_6H_3	−172.7 (2)	4.9 (3)	7.5 (3)	4.83 (13)	–[a]
(II)	2-OH−C_6H_4	anthracen-9-yl	179.1 (2)	2.84 (13)	29.03 (16)	31.35 (8)	KOBXAD[b]
(III)	2-OH−C_6H_4	2-EtOC(=O)CH_2−C_6H_4	173.32 (14)	7.25 (9)	20.02 (9)	27.26 (5)	LOSJIO[c]
(IV)	2,3-$(OH)_2$-4,6-(*t*-Bu)$_2$−C_6H	4-$Me_2NC_6H_4$	−178.09 (12)	10.58 (4)	4.61 (4)	15.03 (3)	EDIQOA[d]
(V)	2-naphthol	4-Me_2N−C_6H_4	−179.8 (2)	2.27 (9)	6.49 (13)	7.84 (6)	EZUYEF[e]
(VI)	2-naphthol	4-OH−C_6H_4	179.30 (16)	3.93 (12)	8.44 (12)	11.91 (6)	RUTGEU[f]
(VII)	2-naphthol	4-Me_2N−C_6H_4	177.98 (15)	4.90 (10)	2.32 (12)	3.82 (6)	RUTFET[g]
(VIII*)	2-naphthol	4-OH-3-MeO-C_6H_4	178.73 (14)	5.78 (10)	15.06 (7)	13.14 (5)	POMNIQ[h]
			177.74 (15)	6.65 (9)	12.05 (11)	18.46 (6)	
(IX)*	2-naphthol	pyren-1-yl	−173 (1)	2.6 (8)	4.4 (7)	6.9 (4)	APACEB[i]
			173 (1)	5.3 (7)	4.7 (7)	7.9 (4)	

* Two independent molecules in the asymmetric unit. References: (*a*) This work; (*b*) Patil & Das (2017); (*c*) Akkurt *et al.* (2015); (*d*) Arsenyev *et al.* (2016); (*e*) Ghosh, Adhikari *et al.* (2016); (*f*) Ghosh, Ta *et al.* (2016); (*g*) Ghosh, Ta *et al.* (2016); (*h*) Kumari *et al.* (2014); (*i*) Ghosh, Ganguly *et al.* (2016)

(I). This number is significantly reduced when H atoms are added to the imine-carbon atoms and examples where a second hydroxy substituent present in the 2-position of the phenyl ring is excluded. Thus, there are eight molecules in the CSD containing the fragment 2-OH-C_6-C(H)=N−N=C(H)-C_6, excluding two calix(4)arene derivatives. While the formation of the hydroxy-O−H···N(imine) bond is common to all molecules, there is a certain degree of conformational flexibility in the molecules as seen in the relevant geometric data collated in Table 5. From the data in Table 5, the molecule reported herein, *i.e.* (I), exhibits the greatest twist about the central N−N bond, whereas virtually no twist is seen in the central C−N−N−C torsion angle for (V), *i.e.* −179.8 (2)°. The dihedral angles between the central C_2N_2 residue and the hydroxy-substituted benzene ring span a range 2.27 (9)°, again in (V), to 10.58 (4)°, for (IV). A significantly greater range is noted in the dihedral angles between C_2N_2 and the second benzene ring, *i.e.* 2.32 (12)° in (VII) to 29.03 (16)° in (II). Accordingly, the greatest deviation from co-planarity among the nine molecules included in Table 5 is found in (II) where the dihedral angle between the outer rings is 31.35 (8)°.

Table 6
Experimental details.

Crystal data	
Chemical formula	$C_{14}H_{10}Cl_2N_2O$
M_r	293.14
Crystal system, space group	Monoclinic, $P2_1/n$
Temperature (K)	296
a, *b*, *c* (Å)	8.5614 (8), 15.6055 (12), 10.0527 (9)
β (°)	95.031 (3)
V (Å^3)	1337.9 (2)
Z	4
Radiation type	Mo *Kα*
μ (mm^{-1})	0.48
Crystal size (mm)	0.35 × 0.30 × 0.30
Data collection	
Diffractometer	Bruker Kappa APEXII CCD
Absorption correction	Multi-scan (*SADABS*; Bruker, 2004)
T_{min}, T_{max}	0.846, 0.867
No. of measured, independent and observed [$I > 2\sigma(I)$] reflections	10171, 3185, 2244
R_{int}	0.023
(sin θ/λ)$_{max}$ (Å^{-1})	0.666
Refinement	
$R[F^2 > 2\sigma(F^2)]$, $wR(F^2)$, *S*	0.044, 0.138, 1.05
No. of reflections	3185
No. of parameters	175
H-atom treatment	H atoms treated by a mixture of independent and constrained refinement
$\Delta\rho_{max}$, $\Delta\rho_{min}$ (e Å^{-3})	0.37, −0.28

Computer programs: *APEX2* and *SAINT* (Bruker, 2004), *SIR92* (Altomare *et al.*, 1994), *SHELXL2014* (Sheldrick, 2015), *ORTEP-3 for Windows* (Farrugia, 2012), *DIAMOND* (Brandenburg, 2006) and *publCIF* (Westrip, 2010).

7. Synthesis and crystallization

Compound (I) was prepared as reported in the literature from the condensation reaction of 2,6-dichlorobenzaldehyde and hydrazine hydrate (Manawar *et al.*, 2019). Crystals in the form of light-yellow blocks for the X-ray study were grown by the slow evaporation of its chloroform solution.

8. Refinement

Crystal data, data collection and structure refinement details are summarized in Table 6. Carbon-bound H-atoms were placed in calculated positions (C−H = 0.93 Å) and were included in the refinement in the riding-model approximation, with U_{iso}(H) set to 1.2U_{eq}(C). The position of the O-bound H atom was refined with U_{iso}(H) set to 1.5U_{eq}(O).

Acknowledgements

The authors thank the Department of Chemistry, Saurashtra University, Rajkot, Gujarat, India, for access to the chemical synthesis laboratory and to the Sophisticated Test and Instrumentation Centre (SITC), Kochi, Kerala, India, for providing the X-ray intensity data.

Funding information

Crystallographic research at Sunway University is supported by Sunway University Sdn Bhd (grant No. STR-RCTR-RCCM-001-2019).

References

Akkurt, M., Mague, J. T., Mohamed, S. K., Ahmed, E. A. & Albayati, M. R. (2015). *Acta Cryst.* E**71**, o70–o71.

Altomare, A., Cascarano, G., Giacovazzo, C., Guagliardi, A., Burla, M. C., Polidori, G. & Camalli, M. (1994). *J. Appl. Cryst.* **27**, 435.

Arsenyev, M. V., Khamaletdinova, N. M., Baranov, E. V., Chesnokov, S. A. & Cherkasov, V. K. (2016). *Russ. Chem. Bull.* **65**, 1805–1813.

Brandenburg, K. (2006). *DIAMOND*. Crystal Impact GbR, Bonn, Germany.

Bruker (2004). *APEX2*, *SAINT* and *SADABS*. Bruker AXS Inc., Madison, Wisconsin, USA.

Farrugia, L. J. (2012). *J. Appl. Cryst.* **45**, 849–854.

Ghosh, A., Adhikari, S., Ta, S., Banik, A., Dangar, T. K., Mukhopadhyay, S. K., Matalobos, J. S., Brandão, P., Félix, V. & Das, D. (2016). *Dalton Trans.* **45**, 19491–19499.

Ghosh, A., Ta, S., Ghosh, M., Karmakar, S., Banik, M., Dangar, T. K., Mukhopadhyay, S. K. & Das, D. (2016). *Dalton Trans.* **45**, 599–606.

Ghosh, S., Ganguly, A., Uddin, M. R., Mandal, S., Alam, M. A. & Guchhait, N. (2016). *Dalton Trans.* **45**, 11042–11051.

Groom, C. R., Bruno, I. J., Lightfoot, M. P. & Ward, S. C. (2016). *Acta Cryst.* B**72**, 171–179.

Kumari, B., Ghosh, A. & Das, D. (2014). Private communication (refcode: POMNIQ). CCDC, Cambridge, England.

Labidi, N. S. (2013). *Int. J. Metals*, Article ID 964328 (5 pages).

Manawar, R. B., Gondaliya, M. B., Mamtora, M. J. & Shah, M. K. (2019). World *Sci. News* 126, 222–247.

Patil, S. K. & Das, D. (2017). *Chem. Select* **2**, 6178–6186.

Sheldrick, G. M. (2015). *Acta Cryst.* C**71**, 3–8.

Spek, A. L. (2009). *Acta Cryst.* D**65**, 148–155.

Tan, S. L., Jotani, M. M. & Tiekink, E. R. T. (2019). *Acta Cryst.* E**75**, 308–318.

Tian, B., He, M., Tan, Z., Tang, S., Hewlett, I., Chen, S., Jin, Y. & Yang, M. (2011). *Chem. Biol. Drug Des.* **77**, 189–198.

Tian, B., He, M., Tang, S., Hewlett, I., Tan, Z., Li, J., Jin, Y. & Yang, M. (2009). *Bioorg. Med. Chem. Lett.* **19**, 2162–2167.

Turner, M. J., Mckinnon, J. J., Wolff, S. K., Grimwood, D. J., Spackman, P. R., Jayatilaka, D. & Spackman, M. A. (2017). *Crystal Explorer 17*. The University of Western Australia.

Westrip, S. P. (2010). *J. Appl. Cryst.* **43**, 920–925.

supporting information

Acta Cryst. (2019). E**75**, 1423-1428 [https://doi.org/10.1107/S2056989019012349]

2-{(1*E*)-[(*E*)-2-(2,6-Dichlorobenzylidene)hydrazin-1-ylidene]methyl}phenol: crystal structure, Hirshfeld surface analysis and computational study

Rohit B. Manawar, Mitesh B. Gondaliya, Manish K. Shah, Mukesh M. Jotani and Edward R. T. Tiekink

Computing details

Data collection: *APEX2* (Bruker, 2004); cell refinement: *APEX2*/*SAINT* (Bruker, 2004); data reduction: *SAINT* (Bruker, 2004); program(s) used to solve structure: *SIR92* (Altomare *et al.*, 1994); program(s) used to refine structure: *SHELXL2014* (Sheldrick, 2015); molecular graphics: *ORTEP-3 for Windows* (Farrugia, 2012) and *DIAMOND* (Brandenburg, 2006); software used to prepare material for publication: *publCIF* (Westrip, 2010).

2-{(1*E*)-[(*E*)-2-(2,6-Dichlorobenzylidene)hydrazin-1-\ ylidene]methyl}phenol

Crystal data

$C_{14}H_{10}Cl_2N_2O$
$M_r = 293.14$
Monoclinic, $P2_1/n$
$a = 8.5614$ (8) Å
$b = 15.6055$ (12) Å
$c = 10.0527$ (9) Å
$\beta = 95.031$ (3)°
$V = 1337.9$ (2) Å^3
$Z = 4$
$F(000) = 600$
$D_x = 1.455$ Mg m^{-3}
Mo $K\alpha$ radiation, $\lambda = 0.71073$ Å
Cell parameters from 4447 reflections
$\theta = 4.8$–$56.3°$
$\mu = 0.48$ mm^{-1}
$T = 296$ K
Block, light-yellow
0.35 × 0.30 × 0.30 mm

Data collection

Bruker Kappa APEXII CCD diffractometer
Radiation source: X-ray tube
ω and φ scan
Absorption correction: multi-scan (SADABS; Bruker, 2004)
$T_{min} = 0.846$, $T_{max} = 0.867$
10171 measured reflections
3185 independent reflections
2244 reflections with $I > 2\sigma(I)$
$R_{int} = 0.023$
$\theta_{max} = 28.3°$, $\theta_{min} = 2.6°$
$h = -11 \rightarrow 11$
$k = -15 \rightarrow 20$
$l = -11 \rightarrow 12$

Refinement

Refinement on F^2
Least-squares matrix: full
$R[F^2 > 2\sigma(F^2)] = 0.044$
$wR(F^2) = 0.138$
$S = 1.05$
3185 reflections
175 parameters
0 restraints
Primary atom site location: structure-invariant direct methods
Secondary atom site location: difference Fourier map
Hydrogen site location: mixed
H atoms treated by a mixture of independent and constrained refinement

$w = 1/[\sigma^2(F_o^2) + (0.069P)^2 + 0.4482P]$
where $P = (F_o^2 + 2F_c^2)/3$
$(\Delta/\sigma)_{max} < 0.001$

$\Delta\rho_{max} = 0.37$ e Å^{-3}
$\Delta\rho_{min} = -0.28$ e Å^{-3}

Special details

Geometry. All esds (except the esd in the dihedral angle between two l.s. planes) are estimated using the full covariance matrix. The cell esds are taken into account individually in the estimation of esds in distances, angles and torsion angles; correlations between esds in cell parameters are only used when they are defined by crystal symmetry. An approximate (isotropic) treatment of cell esds is used for estimating esds involving l.s. planes.

Fractional atomic coordinates and isotropic or equivalent isotropic displacement parameters (Å²)

	x	*y*	*z*	U_{iso}*/U_{eq}
Cl1	0.37913 (8)	−0.06610 (4)	0.23254 (7)	0.0669 (2)
Cl2	0.90894 (8)	−0.10632 (4)	0.57108 (7)	0.0646 (2)
O1	0.8423 (2)	0.25607 (11)	0.52671 (19)	0.0636 (5)
H3O	0.808 (4)	0.206 (2)	0.501 (3)	0.095*
N1	0.66249 (19)	0.14415 (10)	0.39038 (17)	0.0395 (4)
N2	0.6061 (2)	0.06313 (10)	0.34827 (19)	0.0462 (5)
C1	0.7508 (2)	0.31651 (12)	0.4623 (2)	0.0406 (5)
C2	0.6261 (2)	0.29483 (12)	0.36883 (19)	0.0343 (4)
C3	0.5366 (3)	0.36160 (13)	0.3082 (2)	0.0449 (5)
H3	0.4534	0.3486	0.2457	0.054*
C4	0.5688 (3)	0.44563 (15)	0.3390 (2)	0.0555 (6)
H4	0.5073	0.4890	0.2984	0.067*
C5	0.6932 (3)	0.46555 (14)	0.4305 (3)	0.0590 (7)
H5	0.7160	0.5226	0.4505	0.071*
C6	0.7839 (3)	0.40175 (14)	0.4924 (3)	0.0535 (6)
H6	0.8671	0.4158	0.5543	0.064*
C7	0.5859 (2)	0.20707 (12)	0.3350 (2)	0.0378 (4)
H7	0.5026	0.1960	0.2716	0.045*
C8	0.6741 (2)	0.00413 (12)	0.4161 (2)	0.0397 (5)
H8	0.7496	0.0206	0.4834	0.048*
C9	0.6461 (2)	−0.08822 (11)	0.39956 (18)	0.0333 (4)
C10	0.5215 (2)	−0.12658 (13)	0.3210 (2)	0.0389 (5)
C11	0.5039 (3)	−0.21481 (14)	0.3119 (2)	0.0453 (5)
H11	0.4196	−0.2381	0.2594	0.054*
C12	0.6111 (3)	−0.26778 (13)	0.3805 (2)	0.0487 (5)
H12	0.5998	−0.3269	0.3734	0.058*
C13	0.7354 (3)	−0.23366 (13)	0.4599 (2)	0.0459 (5)
H13	0.8080	−0.2694	0.5064	0.055*
C14	0.7504 (2)	−0.14562 (12)	0.4692 (2)	0.0387 (5)

Atomic displacement parameters (Å²)

	U^{11}	U^{22}	U^{33}	U^{12}	U^{13}	U^{23}
Cl1	0.0580 (4)	0.0514 (4)	0.0850 (5)	−0.0036 (3)	−0.0299 (3)	0.0108 (3)
Cl2	0.0631 (4)	0.0443 (3)	0.0800 (5)	0.0068 (3)	−0.0304 (3)	−0.0017 (3)
O1	0.0630 (11)	0.0375 (8)	0.0835 (13)	0.0107 (8)	−0.0322 (9)	−0.0042 (8)

N1	0.0445 (9)	0.0262 (8)	0.0470 (10)	0.0012 (7)	−0.0009 (8)	0.0012 (7)
N2	0.0586 (11)	0.0274 (8)	0.0503 (11)	−0.0011 (8)	−0.0076 (9)	−0.0015 (7)
C1	0.0429 (11)	0.0321 (10)	0.0461 (12)	0.0060 (8)	0.0000 (9)	−0.0012 (8)
C2	0.0393 (10)	0.0284 (9)	0.0356 (10)	0.0048 (8)	0.0047 (8)	0.0015 (8)
C3	0.0543 (12)	0.0381 (11)	0.0414 (11)	0.0098 (9)	−0.0003 (10)	0.0031 (9)
C4	0.0782 (17)	0.0357 (11)	0.0520 (14)	0.0177 (11)	0.0023 (12)	0.0066 (10)
C5	0.0847 (18)	0.0287 (10)	0.0629 (15)	0.0041 (11)	0.0026 (13)	−0.0043 (10)
C6	0.0620 (15)	0.0364 (11)	0.0598 (14)	−0.0004 (10)	−0.0085 (12)	−0.0088 (10)
C7	0.0413 (10)	0.0338 (10)	0.0373 (10)	0.0012 (8)	−0.0020 (8)	0.0001 (8)
C8	0.0389 (10)	0.0315 (9)	0.0478 (12)	−0.0012 (8)	−0.0020 (9)	0.0005 (9)
C9	0.0376 (10)	0.0292 (9)	0.0333 (10)	0.0001 (7)	0.0051 (8)	0.0013 (7)
C10	0.0419 (11)	0.0359 (10)	0.0381 (10)	−0.0009 (8)	−0.0005 (8)	0.0033 (8)
C11	0.0551 (13)	0.0380 (11)	0.0424 (12)	−0.0082 (9)	0.0017 (10)	−0.0042 (9)
C12	0.0688 (15)	0.0285 (10)	0.0496 (13)	−0.0054 (10)	0.0106 (11)	−0.0019 (9)
C13	0.0608 (14)	0.0309 (10)	0.0459 (12)	0.0078 (9)	0.0041 (10)	0.0041 (9)
C14	0.0444 (11)	0.0331 (10)	0.0382 (11)	0.0016 (8)	0.0021 (9)	0.0006 (8)

Geometric parameters (Å, º)

Cl1—C10	1.725 (2)	C5—C6	1.377 (3)
Cl2—C14	1.739 (2)	C5—H5	0.9300
O1—C1	1.354 (2)	C6—H6	0.9300
O1—H3O	0.87 (3)	C7—H7	0.9300
N1—C7	1.281 (2)	C8—C9	1.468 (3)
N1—N2	1.405 (2)	C8—H8	0.9300
N2—C8	1.258 (3)	C9—C14	1.407 (3)
C1—C6	1.388 (3)	C9—C10	1.405 (3)
C1—C2	1.401 (3)	C10—C11	1.387 (3)
C2—C3	1.401 (3)	C11—C12	1.375 (3)
C2—C7	1.445 (3)	C11—H11	0.9300
C3—C4	1.370 (3)	C12—C13	1.379 (3)
C3—H3	0.9300	C12—H12	0.9300
C4—C5	1.380 (4)	C13—C14	1.382 (3)
C4—H4	0.9300	C13—H13	0.9300
C1—O1—H3O	109 (2)	C2—C7—H7	119.3
C7—N1—N2	114.17 (16)	N2—C8—C9	126.41 (18)
C8—N2—N1	111.38 (17)	N2—C8—H8	116.8
O1—C1—C6	117.72 (19)	C9—C8—H8	116.8
O1—C1—C2	121.84 (17)	C14—C9—C10	115.23 (17)
C6—C1—C2	120.44 (19)	C14—C9—C8	118.56 (17)
C3—C2—C1	117.91 (18)	C10—C9—C8	126.20 (17)
C3—C2—C7	119.52 (18)	C11—C10—C9	122.19 (18)
C1—C2—C7	122.57 (17)	C11—C10—Cl1	116.18 (16)
C4—C3—C2	121.5 (2)	C9—C10—Cl1	121.61 (15)
C4—C3—H3	119.3	C12—C11—C10	120.0 (2)
C2—C3—H3	119.3	C12—C11—H11	120.0
C3—C4—C5	119.6 (2)	C10—C11—H11	120.0

C3—C4—H4	120.2	C13—C12—C11	120.35 (18)
C5—C4—H4	120.2	C13—C12—H12	119.8
C6—C5—C4	120.7 (2)	C11—C12—H12	119.8
C6—C5—H5	119.7	C12—C13—C14	119.0 (2)
C4—C5—H5	119.7	C12—C13—H13	120.5
C5—C6—C1	119.9 (2)	C14—C13—H13	120.5
C5—C6—H6	120.1	C13—C14—C9	123.19 (19)
C1—C6—H6	120.1	C13—C14—Cl2	117.00 (16)
N1—C7—C2	121.47 (18)	C9—C14—Cl2	119.80 (14)
N1—C7—H7	119.3		

C7—N1—N2—C8	−172.7 (2)	N2—C8—C9—C14	169.6 (2)
O1—C1—C2—C3	179.3 (2)	N2—C8—C9—C10	−11.4 (4)
C6—C1—C2—C3	−0.3 (3)	C14—C9—C10—C11	−0.6 (3)
O1—C1—C2—C7	0.3 (3)	C8—C9—C10—C11	−179.6 (2)
C6—C1—C2—C7	−179.4 (2)	C14—C9—C10—Cl1	178.08 (15)
C1—C2—C3—C4	−0.2 (3)	C8—C9—C10—Cl1	−0.9 (3)
C7—C2—C3—C4	178.9 (2)	C9—C10—C11—C12	−0.4 (3)
C2—C3—C4—C5	0.8 (4)	Cl1—C10—C11—C12	−179.23 (18)
C3—C4—C5—C6	−0.9 (4)	C10—C11—C12—C13	0.8 (3)
C4—C5—C6—C1	0.3 (4)	C11—C12—C13—C14	0.0 (3)
O1—C1—C6—C5	−179.4 (2)	C12—C13—C14—C9	−1.1 (3)
C2—C1—C6—C5	0.3 (4)	C12—C13—C14—Cl2	179.81 (17)
N2—N1—C7—C2	178.69 (18)	C10—C9—C14—C13	1.4 (3)
C3—C2—C7—N1	−178.4 (2)	C8—C9—C14—C13	−179.5 (2)
C1—C2—C7—N1	0.6 (3)	C10—C9—C14—Cl2	−179.53 (15)
N1—N2—C8—C9	−179.54 (19)	C8—C9—C14—Cl2	−0.5 (3)

Hydrogen-bond geometry (Å, º)

D—H···*A*	*D*—H	H···*A*	*D*···*A*	*D*—H···*A*
O1—H1O···N1	0.87 (3)	1.87 (3)	2.632 (2)	147 (3)